

# We are IntechOpen, the world's leading publisher of Open Access books Built by scientists, for scientists

5,300

Open access books available

130,000

International authors and editors

155M

Downloads

Our authors are among the

154

Countries delivered to

TOP 1%

most cited scientists

12.2%

Contributors from top 500 universities



WEB OF SCIENCE™

Selection of our books indexed in the Book Citation Index  
in Web of Science™ Core Collection (BKCI)

Interested in publishing with us?  
Contact [book.department@intechopen.com](mailto:book.department@intechopen.com)

Numbers displayed above are based on latest data collected.  
For more information visit [www.intechopen.com](http://www.intechopen.com)



# Application of Nd:YAG Laser in Semiconductors' Nanotechnology

Artur Medvid', Aleksandr Mycko, Pavels Onufrijevs and Edvins Dauksta  
*Riga Technical University  
Latvia*

## 1. Introduction

The main tendency in development of modern electronics and optoelectronics is the use of functional objects of small size. Unique properties of the nanoobjects are mainly determined by their atomic and electronic processes occurring in the structure, which has a quantum character.

Surface nanostructures and their unique properties play a significant role in such objects as highly dispersed systems - adsorbents and catalysts, fillers, composite materials, film and membrane systems (Crommie et al., 1993; Beton et al., 1995; Junno et al., 1995). Formation on the surfaces of ordered and disordered ensembles of nanoparticles allow creating materials with new unique physical properties. Nanostructuring of the surface leads to improvement of optical, electrical, thermal, mechanical and field electron emission properties of materials, for example, reducing of the work function of electron from silicon (Evtukh et al., 2010), enhancing biocompatibility with implants in living tissue and prosthetic devices used in orthopaedics and dentistry. Such materials find application in selective nanocatalyse, microelectronics, nanophotonics, photovoltaic, spectroscopy, and optics. On their base devices are created for recording and storing information with ultra-high density, as well as light-emitting devices (Vu et al., 2010).

Study of different mechanisms of nanostructured materials' formation is required due to the need to develop new and effective methods of forming low-dimensional nanostructures when at least one dimension of crystal is less or equal Bohr' radius of electron, hole or exciton. At this condition the quantum confinement effect manifests in the system, and it leads to the essential change of material physical properties.

One promising direction is to use laser radiation to form nanostructures on solid surfaces.

Lasers have been used for more than 50 years in diverse fields of application starting from simple laser micromachining processes for micro-electro-mechanical systems (MEMS), such as, cutting, drilling, to more smarter ones, e.g.: restoration of art works (laser stone cleaning), pulse laser deposition of coatings and films; local defect annealing after ion implantation; formation the precipitation areas of impurities in Si in medicine, medical diagnosis, treatment, or therapy etc.

Among solid state lasers, Nd:YAG laser has an important role due to its high efficiency, possibility to tune it in different wavelengths from infrared ( $\lambda=1064$  nm) till ultraviolet ( $\lambda=213$  nm) and change pulse duration from milliseconds down to picoseconds.

Nowadays, lasers are used for formation of the following semiconductors' structures: p-n junctions, heterostructures Ge/SiGe, CdTe/CdZnTe, and graded band gap (Medvid' & Fedorenko 1999; Medvid', Mychko et al., 2007; Medvid', I.Dmytruk et al., 2007; Medvid', P.Onufrijevs et al., 2008; Medvid', Mychko et al., 2008; Medvid', Onufrijevs et al., 2010; Medvid', Mychko et al., 2010).

Moreover, the most actual application of lasers could be in nanotechnology. We have elaborated a new laser method for nanocones' formation on a surface of semiconductors by laser radiation. The proposed model is characterized by two stages - Laser Redistribution of Atoms (LRA) and Selective Laser Annealing (SLA).

In the case of  $\text{Si}_{0.7}\text{Ge}_{0.3}$  solid solutions the first stage, LRA, is characterized by formation of hetero-structures, such as: Ge/Si due to drift of Ge atoms toward the irradiated surface of the sample in the gradient of temperature, the so-called Thermogradient effect (Medvid', 2002). This process is characterized by positive feedback: after every laser pulse the gradient of temperature increases due to increase of Ge atoms' concentration at the irradiated surface. New Ge phase is formed at the end of the process. Ge atoms are localized at the surface of Si like a thin film. As a result, LRA stage gradually transits to SLA stage.

The second stage, SLA, is characterized by formation of nanocones on the irradiated surface of a semiconductor by selective laser heating of the top layer with a following mechanical plastic deformation of the layer as a result of relaxation of the mechanical compressive stress arising between these layers due to mismatch of their crystal lattices and selective laser heating. SLA occurs due to higher absorption of the laser radiation by the top layer than the buried layer.

In the case of the elementary semiconductors, at the first stage of the process a thin top layer with mechanical compressive stress due to separation and redistribution of interstitials and vacancies in gradient temperature field (Medvid', 2002) on the irradiated surface of the semiconductors is formed. As a result, interstitials are concentrated at the irradiated surface of the semiconductor, forming the top layer. Vacancies are concentrated under the top layer forming a buried layer with mechanical tension due to absence of atoms. Sometimes vacancies form nanocavities (Medvid, 2009). At the second stage of the process nanocones are formed on the irradiated surface of the semiconductors due to plastic deformation of the top layer in the same way as in the previous case with semiconductor solid solutions.

A study of the nanocones' optical, mechanical and electrical properties which are used for construction of third generation solar cells, Si white light emitting diode, photodetector with selective or "bolometer" type spectral sensitivity, Si tip for field electron emitting with low work function of electron is conducted in the chapter.

## **2. Applications of laser redistribution of atoms**

### **2.1 P-n junction formation in i-Ge crystal by laser radiation**

P-n junction is the main component of many semiconductor devices such as diodes, transistors, microchips etc (Makino, Kato, et al. 2008). Thermomodiffusion, ion implantation

(Benda, Gowar, et al. 1999) and molecular beam epitaxy (Tomas, Jennings, et al., 2007) are only a few methods to form a p-n junction. The main drawback for these methods is a high cost per p-n junction, since the equipment for these methods is expensive.

A possibility of p-n junction formation by laser radiation was shown in several p- and n-type semiconductors: p-Si (Mada & Ione, et al., 1986; Blums & Medvid', et al., 1995), p-CdTe (Medvid', Litovchenko et al., 2001), p-InSb (Fujisawa, 1980; Medvid', Fedorenko, et al., 1998), p-InAs (Kurbatov & Stojanova, 1983), p-PbSe (Tovstyuk, Placko, et al., 1984), p-Ge (Kiyak & Savitsky, 1984) and n-HgCdTe (Dumanski, Bester, et al., 2006) due to inversion of conductivity type. Different mechanisms have been proposed to explain the nature of inversion of conductivity type, for example, impurities' segregation, defects' generation (Tovstyuk, Placko, et al., 1984), amorphization (Ljamichev, Litvak, et al. 1976) and oxygen related donor generation (Mada & Ione, et al., 1986). However, n-type impurities in Si irradiated by laser cannot be oxygen atoms, according to paper (Blums & Medvid', et al., 1995). Several authors have tried to explain p-n junction formation in n-type HgCdTe by defects generation, based on a model of defects formation related to interstitial mercury diffusion (Dumanski, Bester, et al., 2006). On the other hand, the authors of those papers did not take into account the effect of temperature gradient on the diffusion of atoms in solid solution. For example, diffusion of Hg interstitials toward the bulk of the semiconductor is impeded due to gradient of temperature directed to the irradiated surface of the semiconductor. Moreover, it is theoretically shown, that the p-n junction can be formed by redistribution of impurities in co-doped Si in gradient temperature field (Medvid' & Kaupuzs, 1994). In this case the atoms with bigger effective radii than Si atom radius drift toward the irradiated surface of the Si crystal, but those with radii smaller than Si atom radius – to the opposite direction.

Characteristics of p-n junction, formed by laser radiation in semiconductors, are comparable to the commercial ones, that is why laser technology has a promising future. The main advantages of this technology are low cost and the possibility to locate p-n junction fast and precisely.

Unfortunately, the mechanism of p-n junction formation by laser radiation has not been clear until now. In this paper a new mechanism of p-n junction formation in intrinsic semiconductor by laser radiation is proposed.

According to the model, p-n junction is formed in a semiconductor by strongly absorbed laser radiation due to generation and redistribution of intrinsic point defects (interstitial atoms and vacancies) in temperature gradient field, so called Thermo gradient effect (Medvid', 2002).

For this purpose i-Ge crystal is irradiated by Nd:YAG laser with different energy of quantum. I-type Ge crystal was used in the experiments as a model material because the concentration of impurities in this material is lower than the concentration of intrinsic point defects at room temperature.

In the experiments i-Ge single crystals with  $N_a = 7.4 \times 10^{11} \text{ cm}^{-3}$ ,  $N_d = 6.8 \times 10^{11} \text{ cm}^{-3}$ , where  $N_a$  and  $N_d$  are acceptors' and donors' concentration, and slab dimensions of  $16.0 \times 3.5 \times 2.0 \text{ mm}^3$  were used. Samples were mechanically polished with diamond paste and chemically treated with  $\text{H}_2\text{O}_2$  and CP-4 ( $\text{HF}:\text{HNO}_3:\text{CH}_3\text{COOH}$  in volume ratio 3:5:3), therefore all surfaces of samples are characterised by minimum surface recombination velocity of  $S_{\text{min}} = 100 \text{ cm/s}$  (Pozela, 1980).

Different intensities and energies of laser radiation quanta:  $h\nu_1=1.16$  eV ( $\lambda_1 = 1064$  nm),  $h\nu_2=2.32$  eV ( $\lambda_2 = 532$  nm), and  $h\nu_4=4.66$  eV ( $\lambda_4 = 266$  nm), where  $\nu_1$ - fundamental frequency,  $\nu_2$ - second harmonics,  $\nu_4$ - fourth harmonics and  $\lambda$ - wavelength, of nanosecond Nd:YAG laser with pulse duration  $\tau_1 = 6.0$  ns,  $\tau_2 = 4.0$  ns and  $\tau_4 = 3.0$  ns, were used to irradiate the samples. Current-voltage characteristics were measured for the non-irradiated and the irradiated samples. Measurements of current-voltage characteristics were done by soldering tin electrical contacts directly on the irradiated surface of i-Ge and on the opposite side. Also, current-voltage characteristics were measured at different number of laser pulses in order to determine the mechanism of the effect. Maximum electric field applied to the samples was 100 V/cm. Measurements of current-voltage characteristics were done at room temperature (T) and atmospheric pressure. Rectification ratio was calculated at constant 30 V voltages.

Current-voltage characteristics of i-Ge samples before and after irradiation by Nd:YAG laser with energy of laser radiation quantum  $h\nu_4=4.66$  eV and different intensities, are shown in Fig. 1. The current-voltage characteristic of the non-irradiated sample is linear. It means, current-voltage characteristics obey Ohm's law and therefore there are no potential barriers between the electric contacts and the sample. But after irradiation by the laser current-voltage characteristics becomes diode-like. Moreover, this process takes place in threshold manner - resistance of the sample increases by 10 times and rectification effect appears at a certain intensity of the laser radiation.

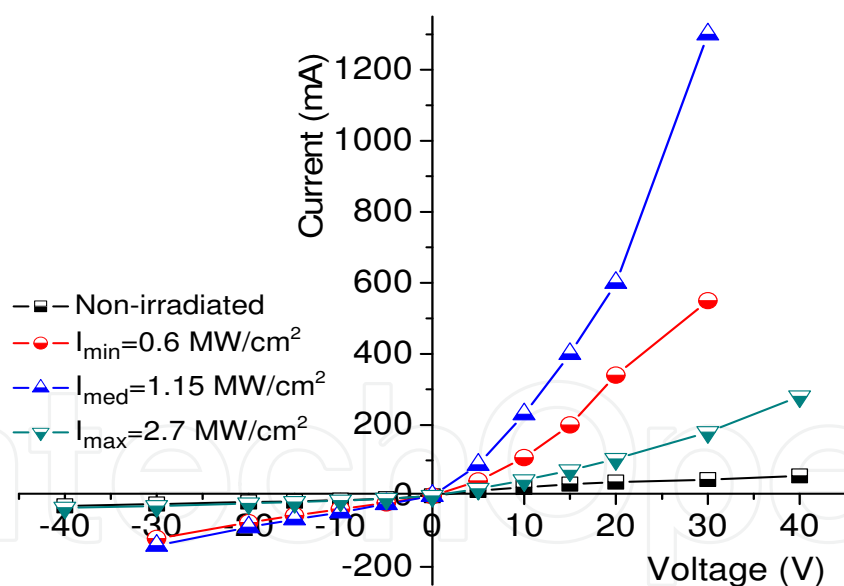


Fig. 1. Current-voltage characteristics of a non-irradiated and an irradiated i-Ge sample by Nd:YAG laser with different intensities of quantum energy  $h\nu_4=4.66$  eV and 350 laser pulses.

Threshold intensity ( $I_{th}$ ) decreases with increase of energy of laser radiation quantum, as seen in Fig. 2. The rectification effect of current-voltage characteristics, quantitatively determined by rectification ratio, is increased with intensity and energy of laser radiation quantum, as shown in Fig. 1. and 2. Threshold intensities are observed at the fundamental frequency  $I_{th1} = 5.5$  MW/cm<sup>2</sup>, the second harmonic  $I_{th2} = 1.5$  MW/cm<sup>2</sup> and the fourth harmonic  $I_{th4} = 1.15$  MW/cm<sup>2</sup>.

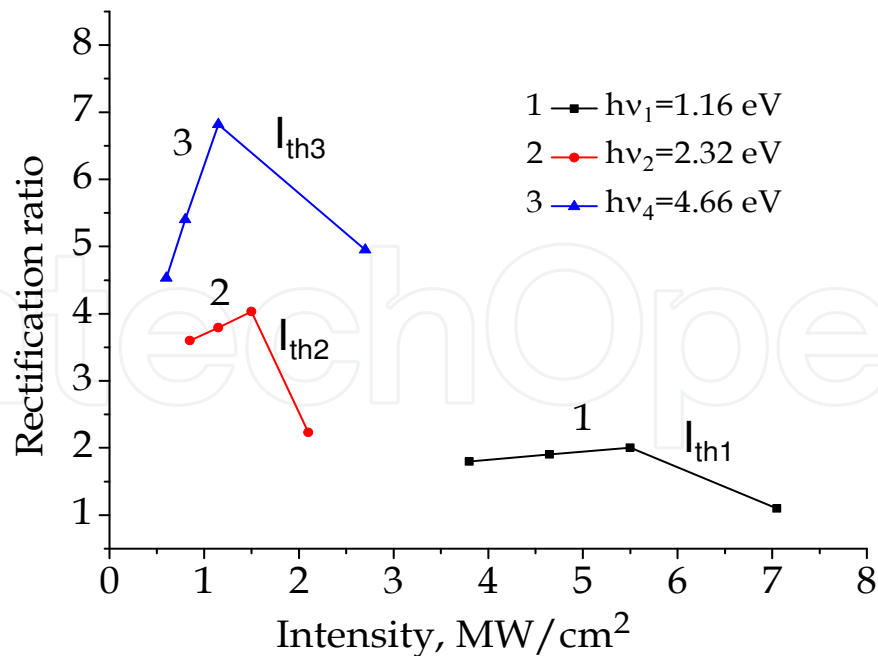


Fig. 2. Rectification ratio as a function of irradiation intensity of Nd:YAG laser for different energies of the laser radiation quantum and 350 laser pulses.

The rectification ratio of 9.3 at 350 laser pulses was observed after irradiation with the highest quantum energy  $h\nu_4=4.66$  eV, but the highest rectification ratio of 400 and potential barrier height 0,472 eV were observed at 650 laser pulses for the second harmonics  $h\nu_2=2.32$  eV as can be seen in Fig. 3.

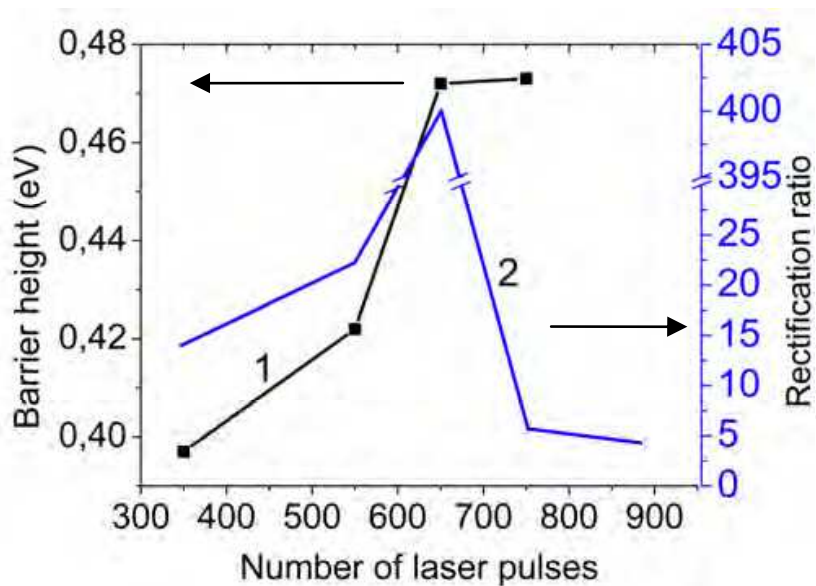


Fig. 3. Barrier height and rectification ratio as a function of number of laser pulses with energy of laser radiation quantum  $h\nu_2=2.32$  eV.

Current-voltage characteristics of samples irradiated with energies of laser radiation quanta  $h\nu_1=1.16$  eV and  $h\nu_2=2.32$  eV are not shown here because they are similar to current-voltage characteristics in Fig. 1. Decrease of the threshold intensity with increase of energy of laser

radiation quantum and appearance of current-voltage characteristics rectification effect we explain in the following way: irradiation of the sample by strongly absorbed laser radiation leads to transformation of the light energy to the thermal one. Heating up the sample by laser radiation increases additional generation of intrinsic defects in crystal - interstitials and vacancies which are quenched in crystal lattice after the end of the laser pulse. The formation of a potential barrier takes place due to separation of vacancies and interstitials in temperature gradient field (Medvid, 2002). Calculations of  $T_{max}$  on the surface of the sample at threshold intensity of laser radiation using the heat balance equation in approach of adiabatic process show that  $T_{max1}$  in the case of fundamental frequency is lower than  $T_{max2}$  for the second and  $T_{max4}$  for the fourth harmonics.

Energy of laser radiation quantum, eV	Wavelength, nm	Absorption coefficient, $\times 10^8 \text{ m}^{-1}$	Absorption depth, $\times 10^{-9} \text{ m}$	Rectification ratio	Barrier height, eV
4,66	266	1.60	6.25	9.29	0.36
2,32	532	0.45	22.2	4.16	0.34
1,16	1064	0.05	200	2.14	0.32

Table 1. i-Ge and p-n junction parameters

It means that gradient of temperature has the main role in formation of the potential barrier, because gradient of  $T$  is proportional to the light absorption coefficient in i-Ge crystal which increases with energy of laser radiation quantum, as seen in Table 1.

Decrease of the threshold intensity of laser radiation with increase of laser radiation quantum, as can be seen in Fig. 2, is an evidence of this suggestion. Concentration of interstitials at the irradiated surface and vacancies in the buried layer of the sample leads to formation of n-p junction because interstitials are donors and vacancies are acceptors in Ge (Shaw, 1973). Schematic illustration of n-p-i structure formed by the laser in i-Ge is shown in Fig. 4.

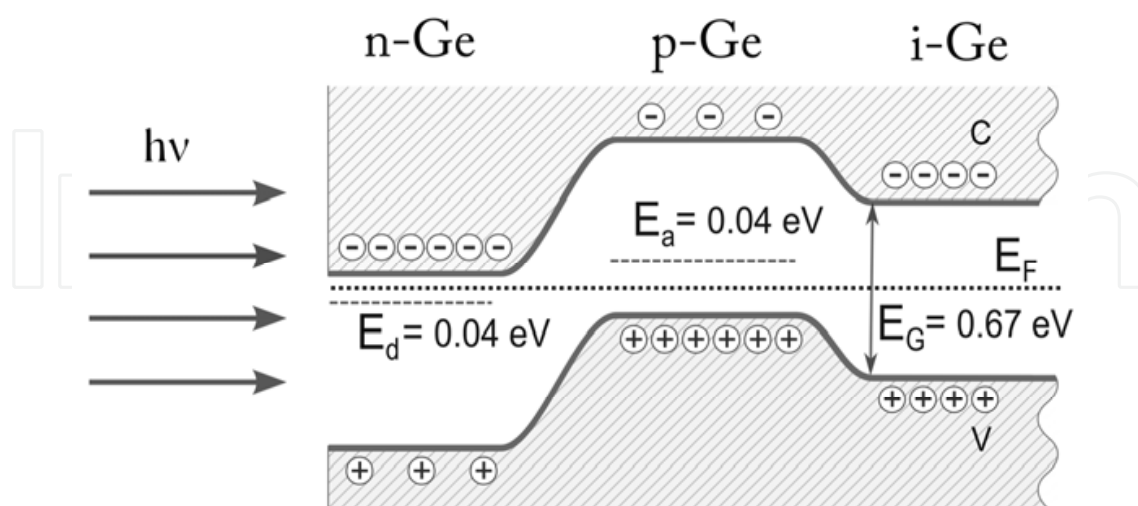


Fig. 4. Schematic illustration of n-p-i structure after irradiation of i-Ge sample. Interstitial atoms are known to be of n-type forming  $E_d$  level 0.04 eV below the conduction band, but vacancies are known to be of p-type forming  $E_a$  level 0.2 eV above the valence band (Claeys & Simon, 2007).

Nonmonotonous dependence of rectification ratio as function of the laser intensity and decrease of rectification ratio at maximal intensities of laser irradiation are explained by formation of nanocones on the irradiated surfaces of the samples (Medvid', Onufrijevs, et al., 2011) and therefore a partial destruction of the n-type layer on the irradiated surface of the samples. The current-voltage characteristics measured at a different number of the laser pulses (N) from 350 to 880 at irradiation of the samples by the second laser harmonic and laser intensity 1.5 MW/cm<sup>2</sup> are shown in Fig. 3. We can see that rectification ratio of the current-voltage characteristics is a non-monotonous function of N with maximum at 650 pulses, as can be seen in Fig.3. At the initial stage of the function rectification ratio increases with N, but at 650 it sharply decreases. Increase of rectification ratio with N (Fig. 3.) we explain by accumulation effect: after every laser pulse concentration of interstitials at the irradiated surface and concentration of vacancies in the buried layer of the sample increases and, of course, n-p junction barrier height increases, too, as shown in Fig. 3, curve 1.

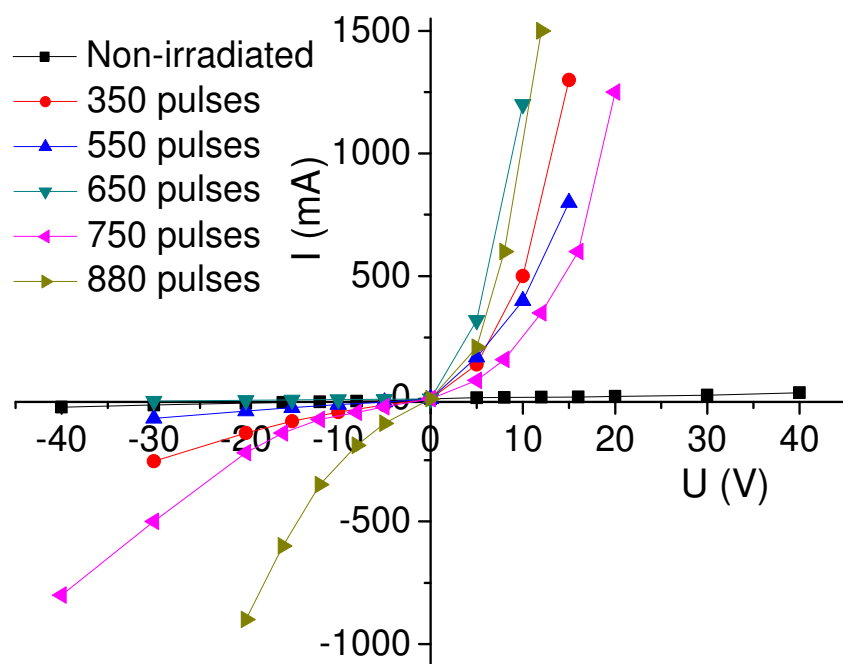


Fig. 5. Current-voltage characteristics of i-Ge samples before and after Nd:YAG laser irradiation at intensity 1.5 MW/cm<sup>2</sup> and quantum energy  $h\nu_2=2.32$  for different number of laser pulses.

To calculate barrier height equation 1 was rearranged to the express barrier height (Gupta, Yakuphanoglu, et al., 2011):

$$I_s = AA^*T^2 \exp\left(-\frac{\phi_b}{kT}\right), \quad (1)$$

where A is the irradiated area ( $0.3 \times 0.3$  cm<sup>2</sup>) of i-Ge, A\* is the Richardson constant, which is 40.8 A cm<sup>-2</sup> K<sup>-2</sup> for i-Ge (Chua, Nikolai, et al., 2003), k is the Boltzmann constant,  $\phi_b$  - the barrier height.

A sharp decrease of rectification ratio at N more than 650 pulses is explained by nanostructure formation on the irradiated surface of the sample due to relaxation of



mechanic compressive stress, as shown in Fig. 6. It arises in the structure due to a high concentration of interstitials in the top layer and vacancies in the buried layer.

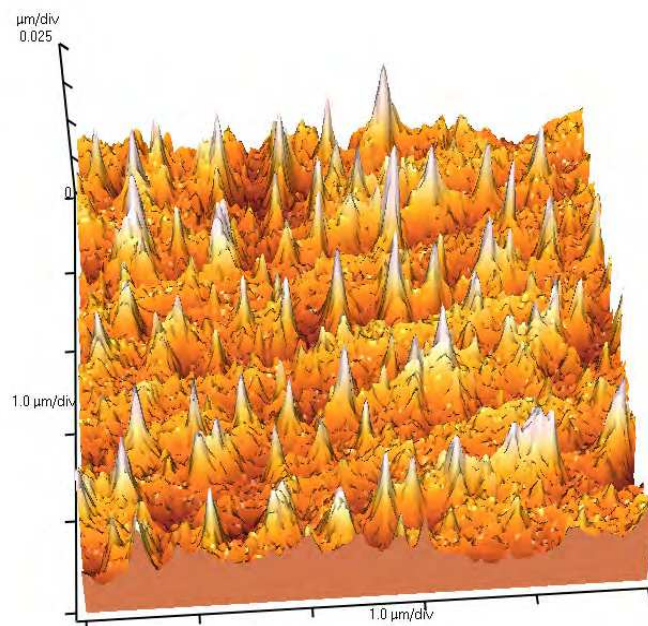


Fig. 6. AFM image of i-Ge surface irradiated by the Nd:YAG laser at intensity 7.0 MW/cm<sup>2</sup>.

### Conclusion

- For the first time we have proved that the mechanism of p-n junction formation in intrinsic semiconductor is caused by generation and redistribution of intrinsic point defects in temperature gradient field.
- Increase of rectification ratio and the potential barrier of p-n junction with the increase of laser radiation intensity and number of the laser pulses are explained by Thermogradient effect, therefore this effect has the main role in formation of p-n junction.

### 2.2 X- and Y-ray detector with increased radiation hardness

It was noted that radiation damage occurs in semiconductor radiation detectors during their operation, while measuring ionizing radiation, which impairs the ability of the device (Lindstrom, 2003). The main expressions of radiation damage are the following: the increase of leakage current in a semiconductor detector, the need to increase the bias voltage, reduction of the efficiency of collecting the charge created by ionization. The main objectives of research are not only the elucidation of the causes of degradation, but also the development of methods for increasing the operation time of devices.

The preliminary irradiation with neutrons or charged particles with subsequent annealing also allows increasing radiation hardness of material.

One of the promising materials for the use in radiation detectors is CdTe and solid solutions based on this material (Fougeres et al., 1999; Niraula et. al., 1999). Due to the wide band gap, detectors based on CdTe can operate at room temperature. One of the important tasks for

application of radiation detectors and semiconductor devices is a study of the possibility to reduce the influence of ionizing radiation on their parameters.

Investigation of influence of  $\gamma$  radiation on the work of CdTe detectors is studied in papers (Franks et. al., 1999; Taguchi et. al., 1978; Cavallini et.al., 2000; Cavallini et.al., 2002). It was noted that CdTe possesses a high enough radiation hardness due to high mass of elements in the compound material (Shapiro, (2002).

In this work the possibility to increase radiation hardness of CdZnTe crystals using laser radiation has been studied.

Single crystals of  $\text{Cd}_{1-x}\text{Zn}_x\text{Te}$  with  $x=0.1$  and sizes  $10.0\text{ mm} \times 10.0\text{ mm} \times 2.0\text{ mm}$  grown by High-Pressure Vertical Zone Melting method were used in our experiments. After irradiation by pulsed Nd:YAG laser samples were  $\gamma$ -irradiated by a  $^{60}\text{Co}$  source ( $E_\gamma$  photons = 1.2 MeV) at room temperature with a dose rate of  $5 \times 10^5\text{ Rad} = 5.0\text{ KGy}$ . Nd:YAG laser with the following parameters: wavelength  $\lambda = 0.532\ \mu\text{m}$ , pulse duration  $\tau = 10.0\text{ ns}$ , power  $P = 1.0\text{ MW}$  and intensity range  $I = 0.48 - 1.80\text{ MW/cm}^2$  was used. The irradiated surface of crystal was covered with a thin layer of  $\text{SiO}_2$  in order to avoid material evaporation during laser irradiation. The thickness of  $\text{SiO}_2$  layer was  $0.3\ \mu\text{m}$  and it was transparent for laser radiation. To assess the damage of the crystalline lattice after irradiation by  $\gamma$ -ray, photoluminescence method was used. Photoluminescence spectra were measured at 5K using 632.8 nm line of He-Ne laser with excitation power of less than 200 mW. It is known that  $\gamma$ -radiation mainly causes intrinsic defect generation in a semiconductor.

Photoluminescence spectra of irradiated and non-irradiated  $\text{Cd}_{1-x}\text{Zn}_x\text{Te}$  crystal by Nd:YAG laser are shown in Figure 7. There are typical photoluminescence spectra of p-type  $\text{Cd}_{0.9}\text{Zn}_{0.1}\text{Te}$  containing an intense band at 1.645 eV ( $A^0X$ ) ascribed to excitons bound to shallow acceptors (Cd vacancies -  $V_{\text{Cd}}$ ), longitudinal optical phonon replicas at 1.624 eV ( $A^0X\text{-LO}$ ) and a weak band at 1.657 eV ( $D^0X$ ) of excitons bound to shallow donors (Cd interstitial -  $\text{Cd}_i$ ). The PL band around 1.54 eV is caused by recombination of donor-acceptor pairs (D-A) with vacancy impurity complexes ( $V_{\text{Cd}}\text{-D}_{\text{Cd}}$ , D=group III or VII elements) (Yang et. al., 2006; Suzuki et. al., 2001).

This non-monotonic change of the intensity of the  $A^0X$  line in photoluminescence can be attributed to the effects of the temperature gradient induced by strong absorption of laser radiation (Thermogradient effect). This effect causes intense generation of point defects and their redistribution in the irradiated area (Medvid', 2002).

Point defects and vacancies are generated under the influence of the temperature gradient in the surface layer during irradiation by laser: Cd ( $V_{\text{Cd}}$ ) vacancies and interstitial atoms of Cd ( $\text{Cd}_i$ ). The increase in  $V_{\text{Cd}}$  concentration causes an increase in the intensity of the  $A^0X$  line in the photoluminescence spectrum. The  $D^0X$  line in the photoluminescence spectrum is not shown, since this semiconductor is initially p-type and therefore the concentration of donors is very small (Figure 7 curves 2 and 3).

After irradiation at high laser intensity generation of point defects in the irradiated area increases. In the irradiated area of semiconductor processes of generation and recombination and simultaneous redistribution of defects in the temperature gradient field take place. Due to the temperature gradient Cd vacancies move in to the bulk of semiconductor in the region of lower temperature, but interstitial atoms of Cd - in the opposite direction, to the surface of semiconductor. When the laser irradiation intensity reaches  $1.2\text{ MW/cm}^2$  gradient of

temperature partially compensates vacancies of Cd atoms by Zn atoms (Figure 7 curve 4). This is due to the greater bonding energy of Zn and Te atoms in comparison to Cd and Te atoms. At lower intensities of laser irradiation, this process is less likely to happen.

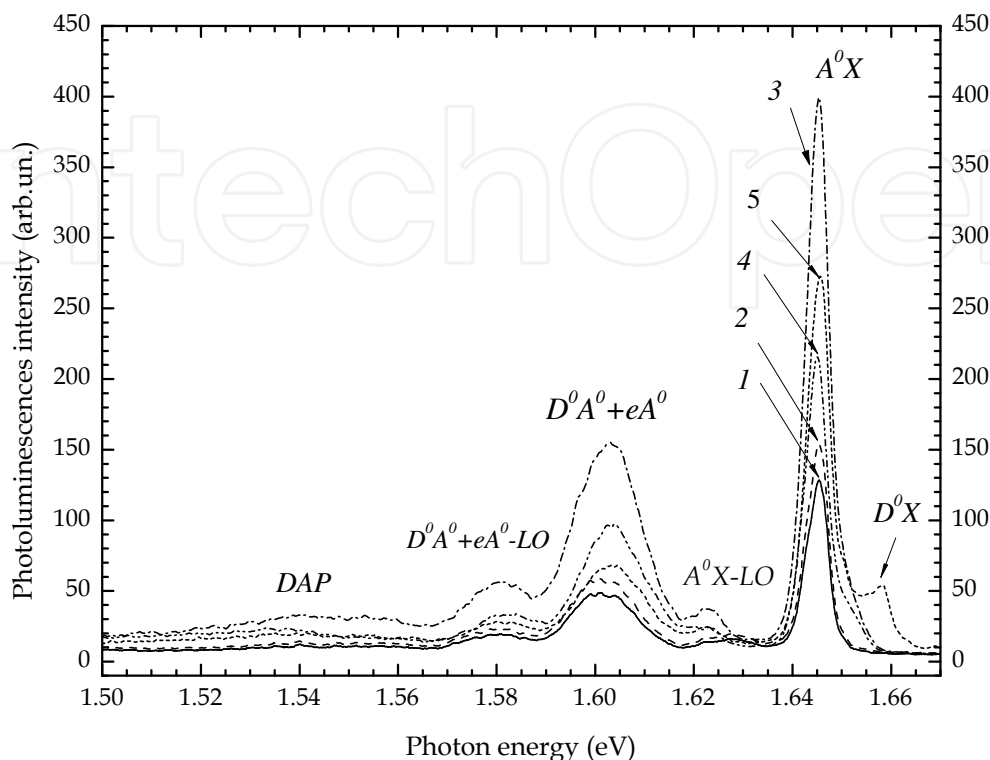


Fig. 7. The photoluminescence intensity as a function of photon energy for  $\text{Cd}_{1-x}\text{Zn}_x\text{Te}$  before and after irradiation by Nd:YAG laser: curve 1 - non irradiated; curve 2 - irradiated with intensity  $0.48 \text{ MW/cm}^2$ ; curve 3 - irradiated with intensity  $0.84 \text{ MW/cm}^2$ ; curve 4 - irradiated with intensity  $1.20 \text{ MW/cm}^2$ ; curve 5 - irradiated with intensity  $1.80 \text{ MW/cm}^2$ .

As a result, the  $A^0X$  line intensity decreases due compensation of vacancies by Zn atoms as well as localization of  $V_{\text{Cd}}$  in the bulk of semiconductor. Intensive generation of interstitial atoms of Cd and increase of their concentration, and their localization at the surface can be proved by appearance of a the  $D^0X$  line in the photoluminescence spectrum (Figure 7 curve 5 and Figure 8 curve 2). Thus, in the surface layer of irradiated semiconductor a region highly enriched by point defects  $V_{\text{Cd}}$  and  $\text{Cd}_\text{I}$  is formed.

Irradiation of  $\text{Cd}_{1-x}\text{Zn}_x\text{Te}$  crystal by  $\gamma$ -ray with a dose rate of  $5 \times 10^5 \text{ Rad} = 5.0 \text{ KGy}$  leads to a strong increase of the  $A^0X$  band intensity in photoluminescence spectra of  $\text{Cd}_{1-x}\text{Zn}_x\text{Te}$  crystal, as shown in Figure 8. For example, intensity of the  $A^0X$  band is increased 10 times for curve 3 in comparison with intensity for curve 1. At the same time, the  $D^0X$  band in photoluminescence spectrum of  $\text{Cd}_{1-x}\text{Zn}_x\text{Te}$  crystal disappears fully, as shown in Figure 9, curve 2 and Figure 10, curve 2.

We explain this effect by Cd vacancies' generation and localization in the excited luminescence thin layer after  $\gamma$ -irradiation of  $\text{Cd}_{1-x}\text{Zn}_x\text{Te}$  crystal.

The main effect observed in the study is suppression of  $V_{\text{Cd}}$  generation and /or localization by  $\gamma$ -radiation at the irradiated surface of  $\text{Cd}_{1-x}\text{Zn}_x\text{Te}$  crystal if the crystal is preliminary irradiated by the laser.

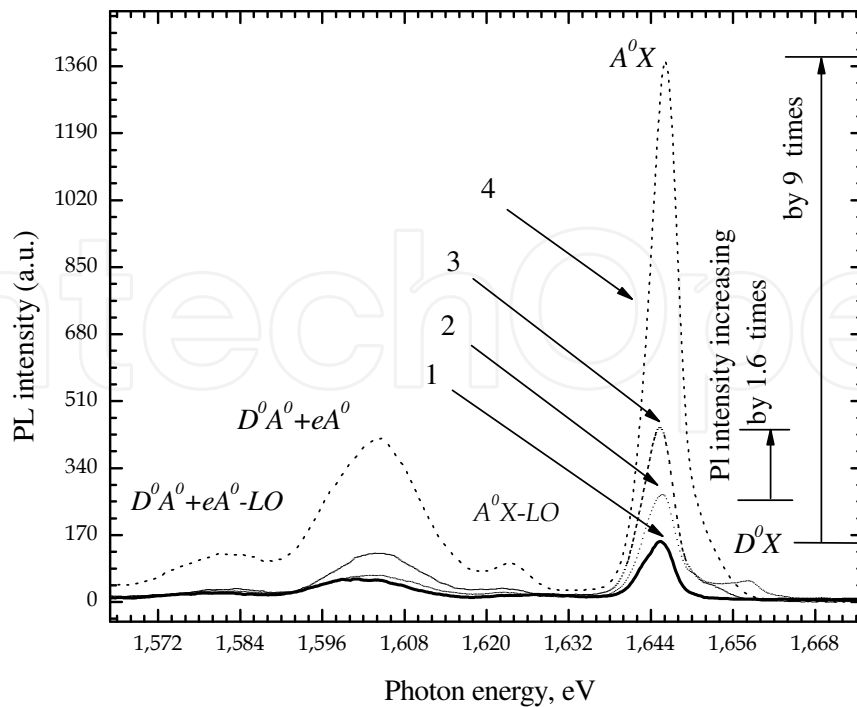


Fig. 8. The photoluminescence spectra of Cd<sub>1-x</sub>Zn<sub>x</sub>Te crystal before (curve 1) and after irradiation by Nd:YAG laser: curve 2 - irradiated by Nd:YAG laser with intensity 1.80 MW/cm<sup>2</sup>; curve 4 - irradiated by  $\gamma$ - ray with a dose rate of 5.0 KGy; curve 3 - previously irradiated by Nd:YAG laser with intensity 1.80 MW/cm<sup>2</sup> and subsequently by  $\gamma$ - ray with a dose rate of 5.0 KGy

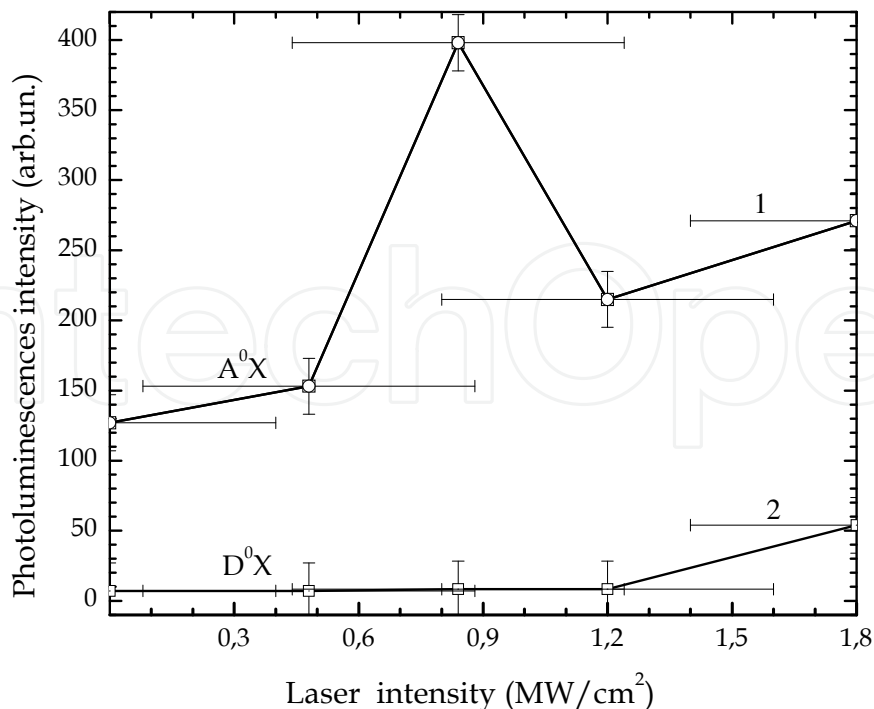


Fig. 9. The photoluminescence intensity of the A<sup>0</sup>X (curve 1) and D<sup>0</sup>X (curve 2) bands of CdZnTe crystal irradiated by the laser as a function of Nd:YAG laser intensity.

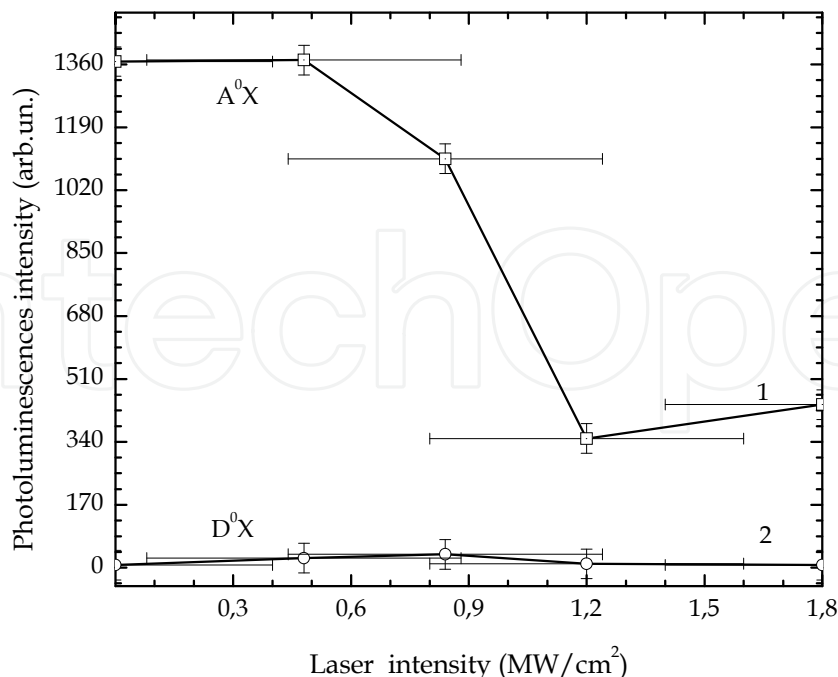


Fig. 10. The photoluminescence intensity of A<sup>0</sup>X (curve 1) and the D<sup>0</sup>X (curve 2) bands of CdZnTe crystal irradiated by the laser and after subsequent irradiation by  $\gamma$ -rays with a dose rate of 5.0 KGy as a function of Nd:YAG laser intensity.

The effect increases with intensity of the laser in region of the laser intensity up to 0.50 - 2.0 MW/cm<sup>2</sup>, as shown in Figure 8, curve 3. This effect is clearly observed in Fig. 3 and Fig.4. Intensity of the A<sup>0</sup>X band in photoluminescence spectrum of Cd<sub>1-x</sub>Zn<sub>x</sub>Te crystal increases only 1.7 times (for comparison, non-irradiated by the laser: 9.3 times) after  $\gamma$ -radiation if the crystal preliminary was irradiated by the laser at intensity 1.2 WM/cm<sup>2</sup>.

Gamma radiation causes the generation of additional Cd vacancies and interstitial Cd atoms, which causes the growth of the intensity of the A<sup>0</sup>X line in the photoluminescence spectrum. Generation and recombination process takes place simultaneously, when the existing interstitial atoms or atoms generated under the influence of gamma radiation move and fill the existing vacancies or newly generated vacancies. As a result, the rate of increase in the concentration of vacancies and interstitial atoms is slowed down because of their partial recombination. These processes can be explained by a decrease of the A<sup>0</sup>X line intensity growth, which also means an increase in radiation resistance of semiconductor.

It should be noted that such mechanism of "defect healing" is valid only up to certain values of radiation doses at which the number of donors formed by laser irradiation may still restrain the growth of the number of vacancies due to the effects of gamma radiation.

### 3. Application of selective laser annealing

#### 3.1 Third generation solar cells on the base of ITO/Si/Al structure

Indium-tin-oxide (ITO) thin films are widely used as a transparent conductive oxide in optoelectronics devices such as solar cells (Bruk *et al.*, 2009), liquid crystal displays and plasma display panels. This material has high transmittance in the visible region of spectra (Adurodija

*et al.*, 2002), surface uniformity and process compatibility (Blasundaraprabhu *et al.*, 2009). ITO is a perspective material for elaboration of new generation solar cells using nanotechnology.

We investigated the ITO/p-Si/Al structure irradiated by Nd:YAG laser with the aim to form a p-n junction and to grow nanocones on the interface of ITO/Si.

ITO/p-Si/Al structures, with ITO top layer thickness of 70 nm, Si layer thickness of 500  $\mu\text{m}$  and an Al back layer thickness of 100 nm in the experiments were studied. The structures were irradiated from the ITO side by Nd:YAG laser second harmonic with a wavelength of  $\lambda = 512$  nm and a pulse duration of  $\tau = 10$  ns. The diameter of the laser beam spot was 0.9

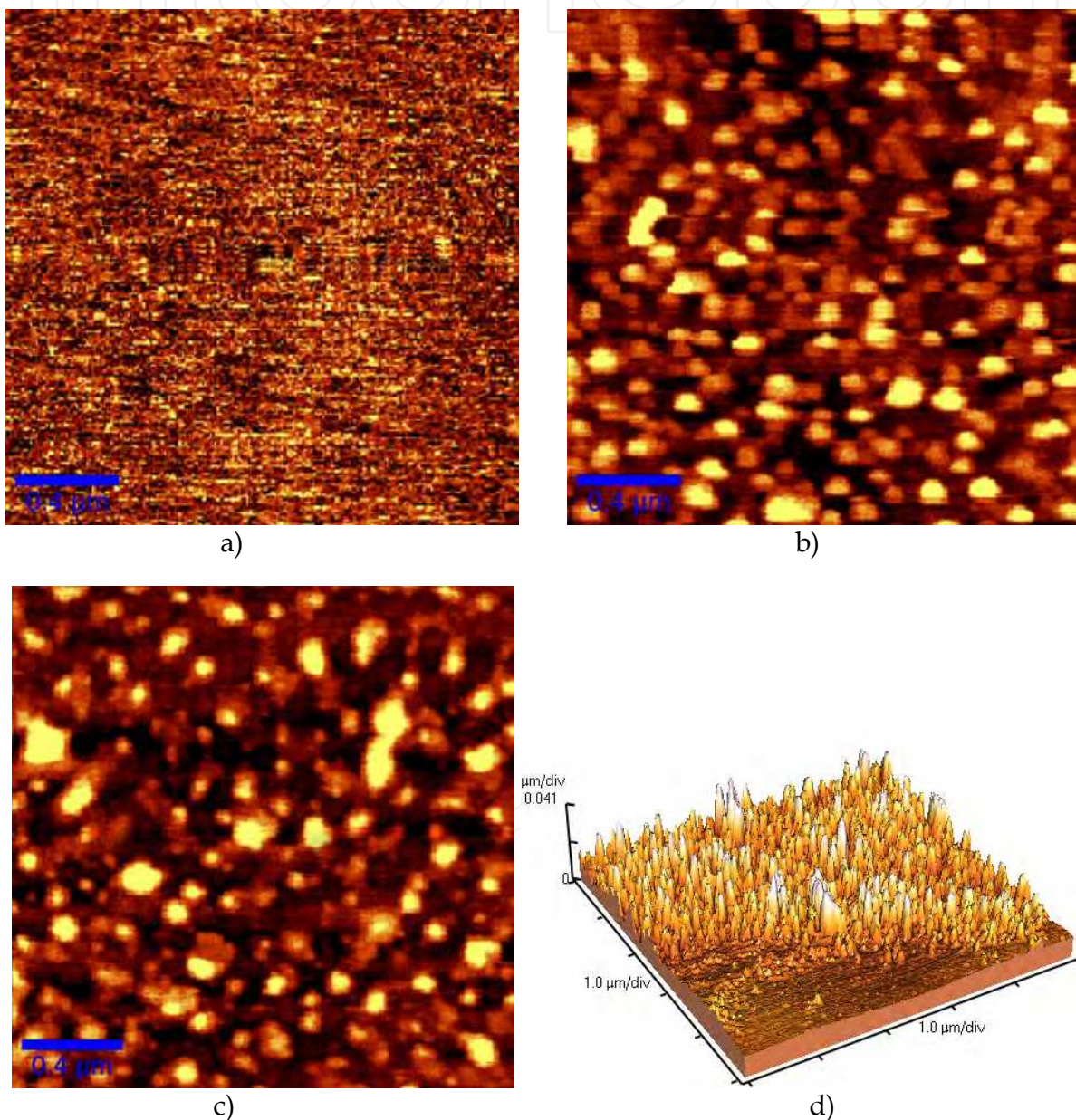


Fig. 11. Atomic force microscope images of ITO/p-Si structure: a) non-irradiated, irradiated by Nd:YAG laser at intensities of b) 1.13 MW/cm<sup>2</sup>; c) 2.83 MW/cm<sup>2</sup> and d) border of non-irradiated (smooth surface) and irradiated by Nd:YAG laser at intensity 2.83 MW/cm<sup>2</sup> (surface with nanocones).

mm. Irradiation of the samples in the scanning regime using a two coordinate manipulator with 20  $\mu\text{m}$  step was carried out. Experiments in ambient atmosphere at pressure of 1 atm,  $T = 20^\circ\text{C}$ , and 60% humidity were performed.

The irradiated structures were studied using atomic force microscope and photoluminescence spectroscopy method. The measurements of current - voltage characteristic to observe the changes of electrical parameters for ITO/p-Si/Al structure after irradiation by laser were carried out. The n-type Si layer was formed on p-type Si, due to drift of interstitial Si atoms towards the irradiated surface, as a result of huge gradient of temperature induced by laser radiation, that so called Thermogradient effect (Medvid', 2002).

The two-dimensional surface topography of ITO/p-Si structure was studied by atomic force microscope, non-irradiated and irradiated by the Nd:YAG laser at intensities of 1.13  $\text{MW}/\text{cm}^2$  and 2.83  $\text{MW}/\text{cm}^2$  (figures 11a, 11b, 11c, respectively). Nanocones were observed on the irradiated Si surface with the average height 12 nm and 26 nm formed by laser radiation at the intensity of 1.13  $\text{MW}/\text{cm}^2$ , and 2.83  $\text{MW}/\text{cm}^2$ , respectively (e.g. see figures 11d).

Photoluminescence spectra of the ITO/p-Si structures with the maxima at 575 nm and 490 nm obtained after laser irradiation at intensities of 1.13  $\text{MW}/\text{cm}^2$  and 2.83  $\text{MW}/\text{cm}^2$  are shown in figure 12. Position of the observed photoluminescence maximum compared with the bulk Si shows a significant "blue shift". The maxima of the photoluminescence band at 575nm and 490 nm are explained by presence of the Quantum confinement effect (Brus, 1984) on the top of nanocones.

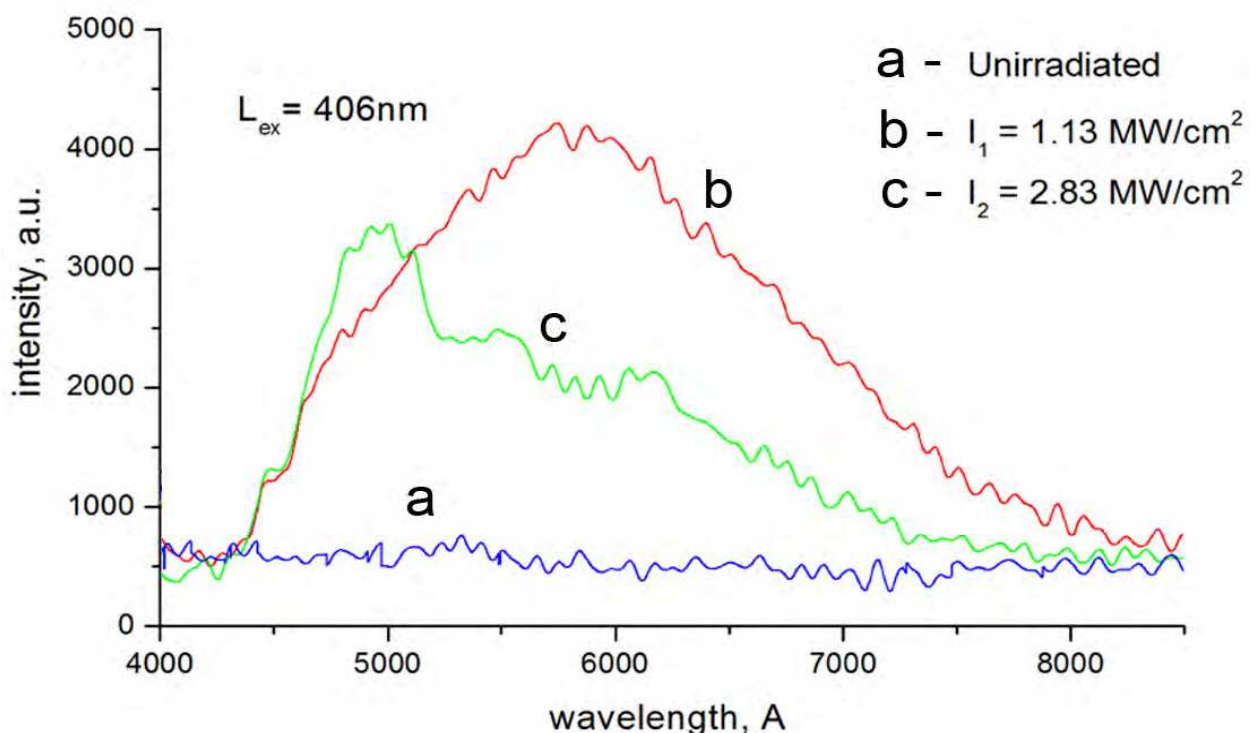


Fig. 12. Photoluminescence spectra of ITO/p-Si structure: before and after irradiation by the Nd:YAG laser.

After irradiation of ITO/p-Si/Al structure by the laser, photocurrent - voltage characteristic measurements (see figure 13) have shown, that electrical power output increased by two

times in comparison to the nonirradiated structure. This effect is explained by increase of absorption coefficient due to quantum confinement effect in nanocones. That means Si band gap is increasing with the increase of laser radiation intensity.

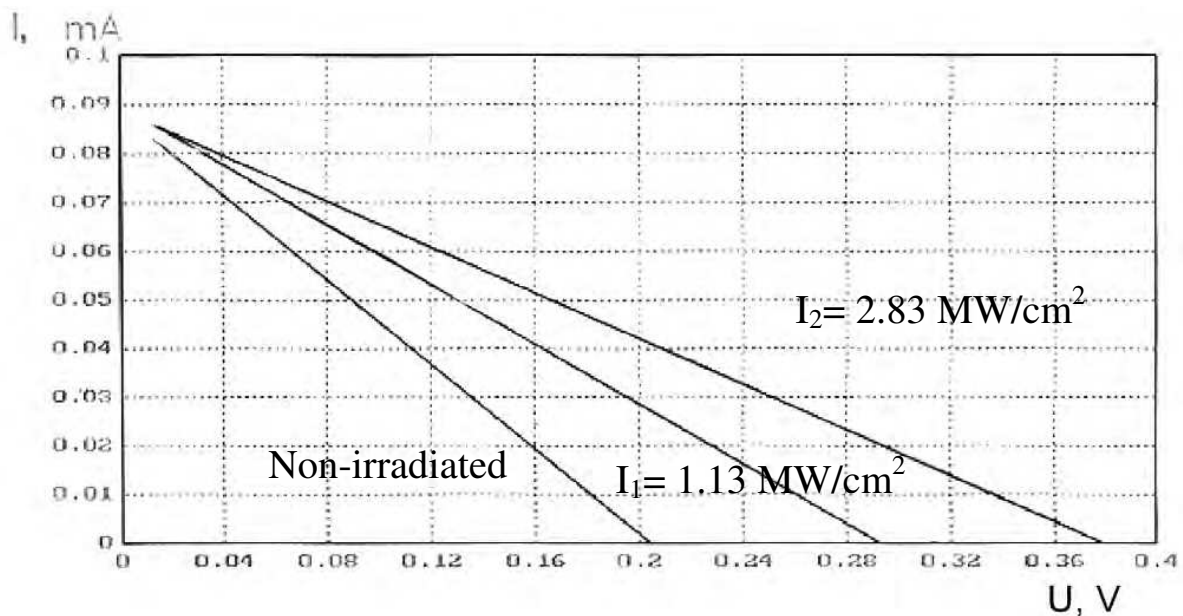


Fig. 13. Photocurrent-voltage characteristic of ITO/p-Si/Al structure before and after irradiation by laser with different intensities.

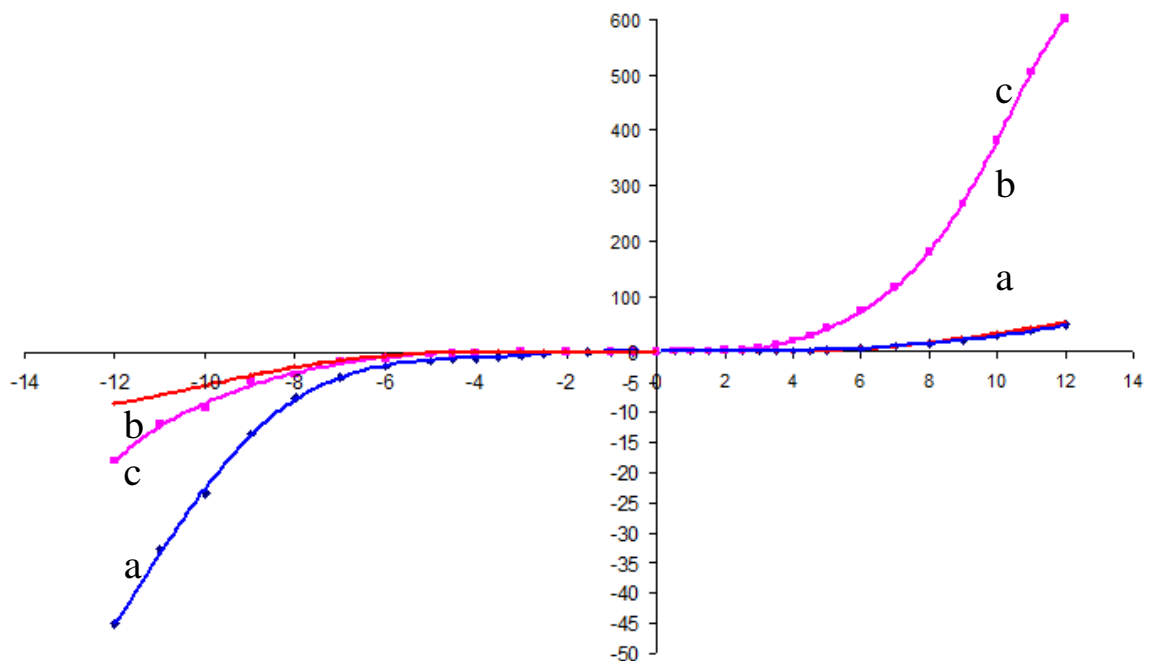


Fig. 14. Dark current-voltage characteristic of ITO/p-Si/Al structure: a) non-irradiated; irradiated by Nd:YAG laser at intensities of b)  $1.13 \text{ MW/cm}^2$ ; c)  $2.83 \text{ MW/cm}^2$ .

It is found that the dark current-voltage characteristic becomes diode-like with rectification coefficient  $K = 10^5$  at 5 V. The result is caused by the laser irradiation with intensity  $I_2 = 2.83$



MW/cm<sup>2</sup> (see figure 14). The improvements of ITO/p-Si/Al structure as a solar cell can be explained by the increase of potential barrier between ITO and p-Si layers.

### Conclusion

- The possibility of p-n junction and Si nanocones' formation by laser irradiation in ITO/p-Si/Al structure was shown.
- The photoluminescence spectra from irradiated ITO/p-Si/Al structure by laser irradiation have been found in visible range of spectra and explained by presence of quantum confinement effect in nanocones with graded band gap.
- Study of the dark current-voltage characteristics showed diode-like character with rectification coefficient  $K = 10^5$  at 5 V caused by laser irradiation with intensity  $I = 2.83$  MW/cm<sup>2</sup>.
- After irradiation of ITO/p-Si/Al structure by laser, the solar cell electrical power output increased by two times in comparison to the nonirradiated structure.

### 3.2 Electron field emitter based on Si nanocones

Silicon electron field emitters may be attractive for numerous applications, mostly due to their compatibility with the dominating Si-based solid state micro- and nanoelectronics.

Nanocones have been formed on the surface of p-Si crystal after irradiation by the second harmonic of Nd:YAG laser with an intensity of 2.0 MW/cm<sup>2</sup> (Evtukh et al., 2010). The measurements of electron field emissions were performed with a flat diode configuration with a glass spacer (figure 15). Distance between the cathode (silicon wafer) and the anode was 0.8 mm. The applied field emission setup allows achieving a vacuum of  $1 \times 10^{-5}$  Pa. The applied voltage varied between 1500-3600 V.

#### Configuration

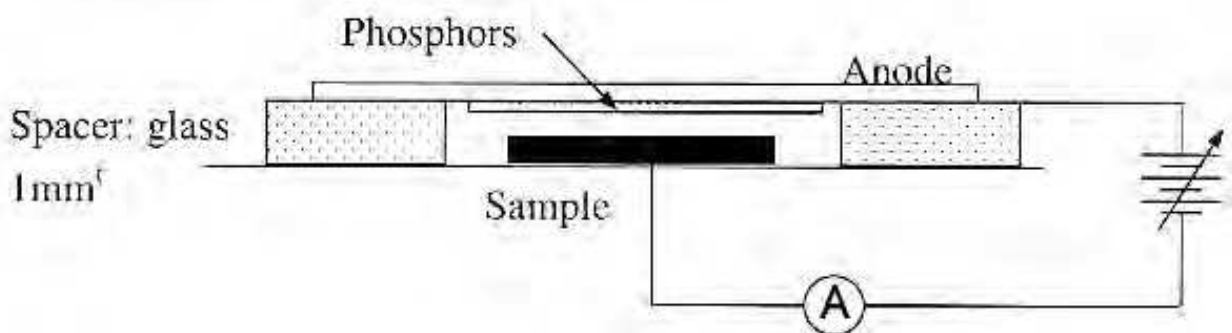


Fig. 15. Cell for electron field emission measurements.

Nanocones with a nanosphere on top of each cone were formed after irradiation by the laser (figure 16). A decrease in the nanosphere diameter from 600 nm to 20 nm with an increase of intensity of laser pulse from 2.0 MW/cm<sup>2</sup> to 20.0 MW/cm<sup>2</sup> was observed. Nanocones have been formed on the irradiated surface of p-Si crystal by second harmonic of Nd:YAG laser with intensity 2.0 MW/cm<sup>2</sup>.

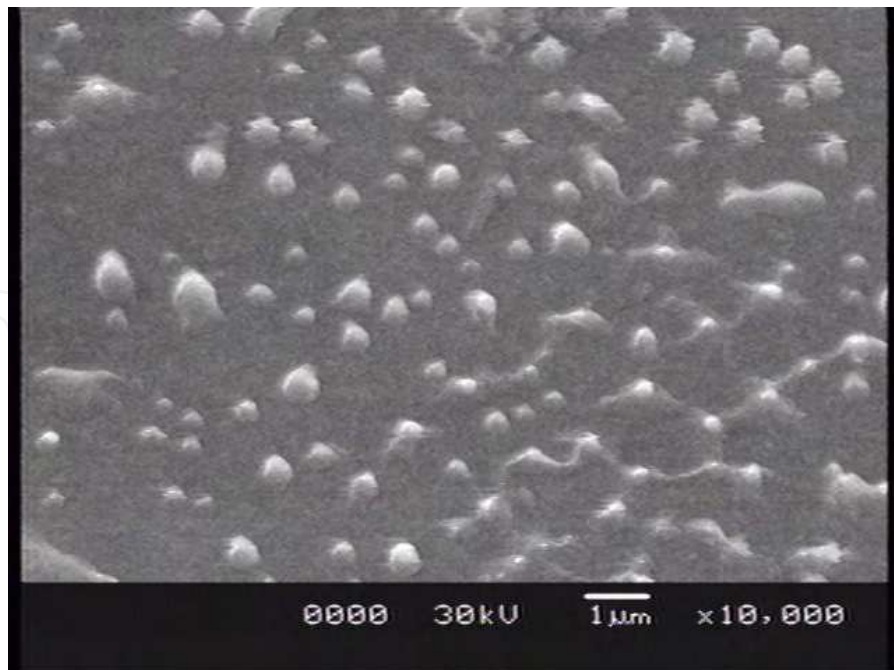


Fig. 16. Scanning electron microscope image of Si nanocones created by laser irradiation.

The electron field emission from such nanocones has some peculiarities, namely: (i) decrease of the threshold field from  $E_{th}=4 \times 10^4$  V/cm at the first measurement to  $E_{th}=3.5 \times 10^4$  V/cm in subsequent measurements, (ii) two slopes of Fowler-Nordheim curves (higher slope at low fields and lower slope at high fields) (figure 17). Analysis of the scanning electron microscope micrographs and electron field emission curves allows us to estimate (i) the electron field enhancement coefficient,  $\beta \approx 100$ , (ii) work functions ( $\Phi_1=6.8$  eV at the first

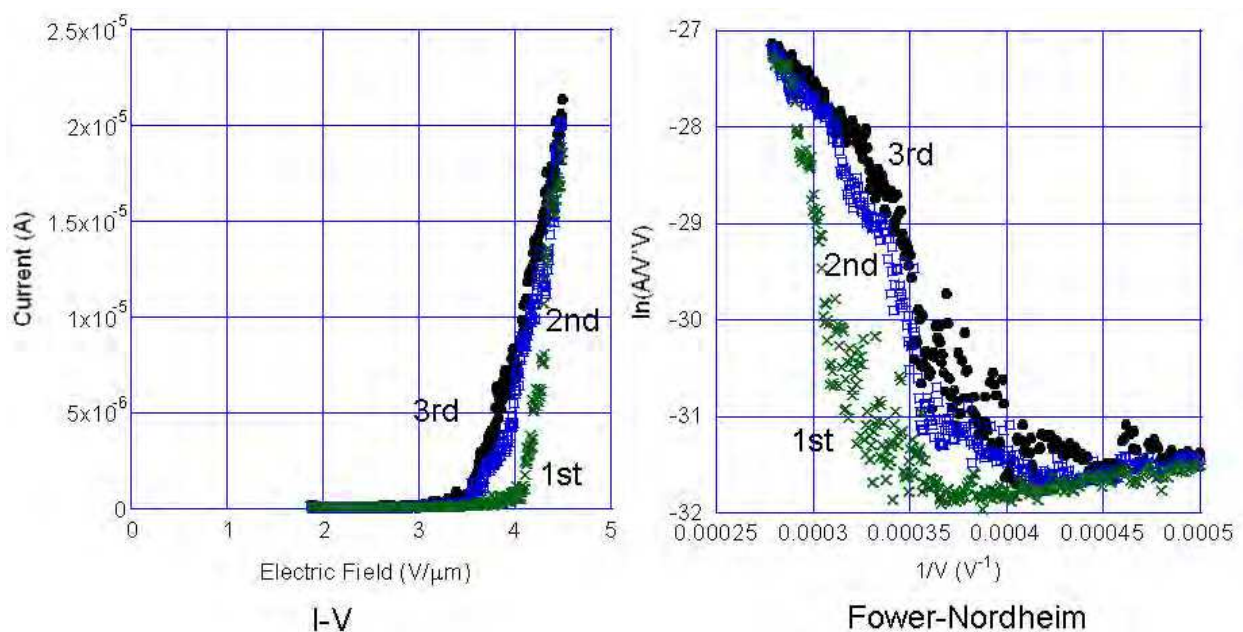


Fig. 17. Current-voltage characteristics (a) and corresponding Fowler-Nordheim plots (b) of Si nanocones electron field emission. Nanocones have been formed by second harmonic of Nd:YAG laser with intensity  $2.0 \text{ MW/cm}^2$ .

measurement and  $\Phi_2=3.9$  eV,  $\Phi_3=2.38$  eV from the two slopes in subsequent measurements), (iii) effective emission area,  $\alpha=3\times 10^{-8}$ - $1.8\times 10^{-5}$  cm<sup>2</sup>. The lower work function in relation to the known value for high doped n-type silicon  $\Phi_0=4.15$  eV we explain by increase of Si band gap on the top of nanocones.

### 3.3 High intensity Si source of white light and photodetector with selective or “bolometer” type of spectral sensitivity on the base of nanocones

A result of investigation of photoluminescence spectra of Si and  $\text{Ge}_x\text{Si}_{1-x}$  crystals has shown (figures 18 and 19), that nanocone radiate wide spectrum of light like sun or glow lamp. At the same time, this structure can be used as photon detector with “bolometer” type of spectral photo sensitivity (Capasso Federico, 1987), as shown in figure 20, curve 1, if irradiation of the structure takes place from the wide band gap part of semiconductor with gradient band gap structure, it means from top of cones, or as photon detector with selective type of spectral photo sensitivity, if irradiation of the structure takes place from narrow band gap part of graded band gap structure, as shown in figure 20, curve 2.

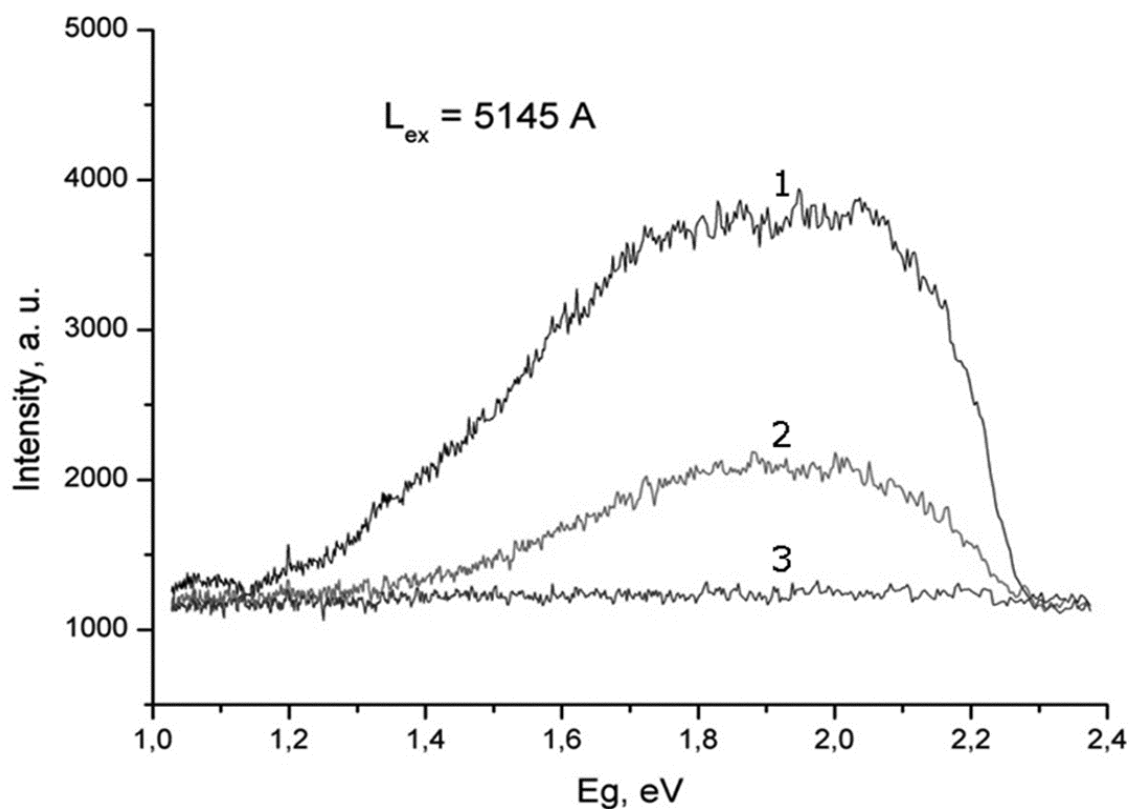


Fig. 18. Photoluminescence spectra of the  $\text{SiO}_2/\text{Si}$  structure irradiated by the laser at intensity  $2.0 \text{ MW}/\text{cm}^2$  (2. and 3. curves), after removing of  $\text{SiO}_2$  layer by chemical etching in HF acid (3. curve). 1. curve corresponds to photoluminescence of the non-irradiated surface.

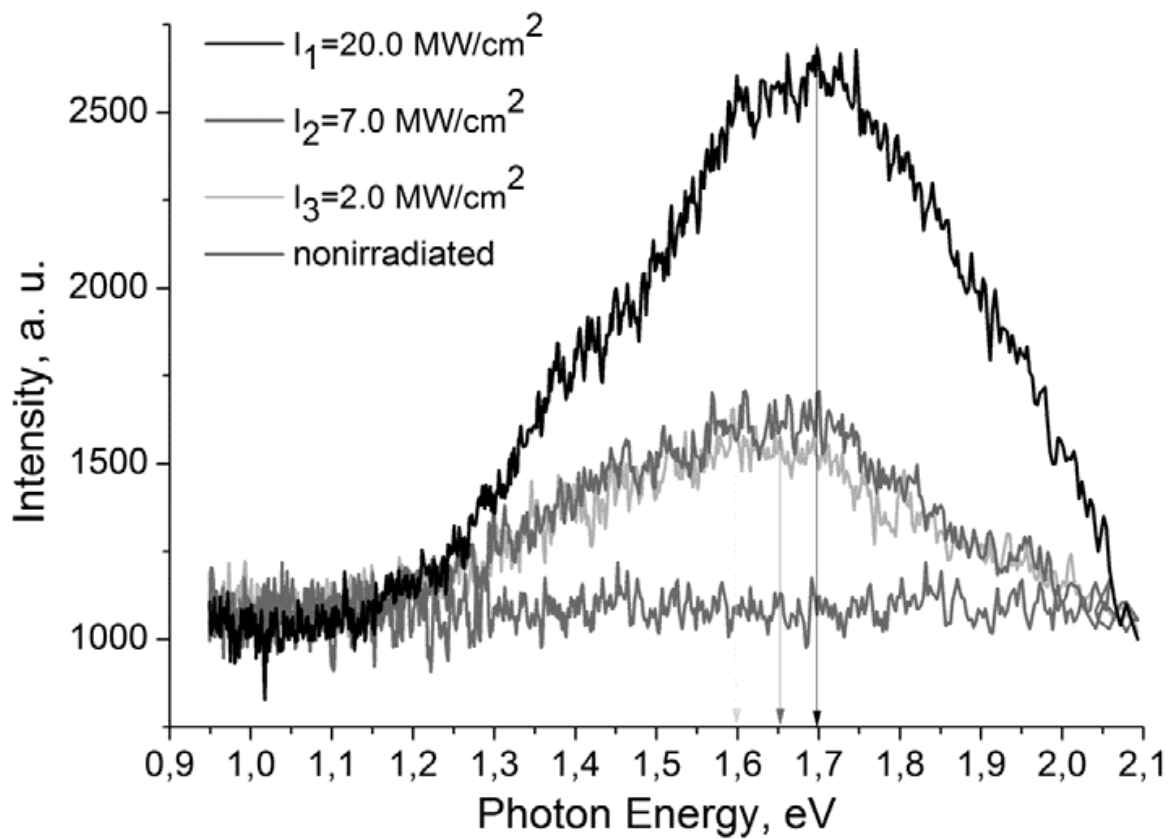


Fig. 19. Photoluminescence spectra of  $\text{Si}_{0.7}\text{Ge}_{0.3}/\text{Si}$  heteroepitaxial structures before and after irradiation by Nd:YAG laser.

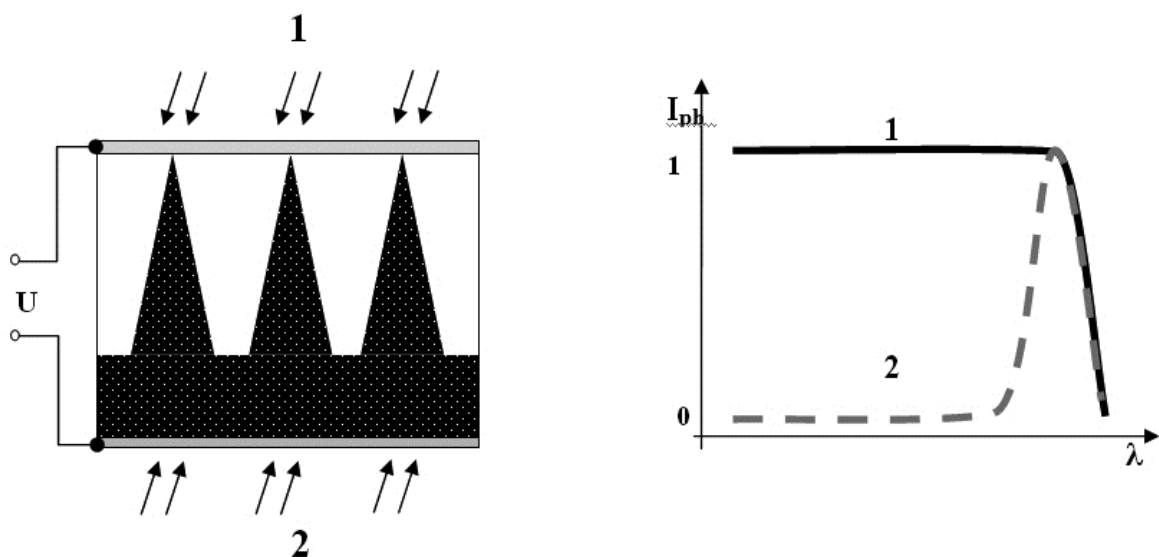


Fig. 20. Scheme of photodetector with graded band gap structure and photoconductivity spectra of photodetector with "bolometric" type of photo sensitivity - curve 1 (detector irradiated from nanocones' side 1) and photodetector with selective type photo sensitivity - curve 2 (detector irradiated from base side 2).

#### 4. Summary

Two-stage mechanism of nanocones' formation on a surface of semiconductor by Nd:YAG laser radiation consists of Laser Redistribution of Atoms and Selective Laser Annealing. This model was successfully applied for explaining p-n junction formation in i-Ge, increase of radiation hardness, formation of nanocones by laser radiation.

Power output of ITO/p-Si/Al solar cell structure has been increased by two times after irradiation by Nd:YAG laser second harmonic with intensity 2.83 MW/cm<sup>2</sup> due to formation of Si nanocones with p-n junction on their top. Decrease by two times of work function of electrons from Si nanocones formed by Nd:YAG laser second harmonic with intensity 2.0 MW/cm<sup>2</sup> is explained by increase of Si band gap on the top of nanocones due to quantum confinement effect.

#### 5. Acknowledgment

The author gratefully acknowledges financial support in part by Europe Project in the framework FR7-218000 "COCAE", European Regional Development Fund within the project "Sol-gel and laser technologies for the development of nanostructures and barrier structures", the ESF Projects No. 1DP/1.1.1.2.0/09/ APIA/VIAA/142 and «Support for the implementation of doctoral studies at Riga Technical University».

#### 6. References

- Adurodija F.O.; Izumi H.; Ishihara T.; Yoshioka H.; Motoyama M. & Murai K. (2002). Effect of laser irradiation on the properties of indium tin oxide films deposited at room temperature by pulsed laser deposition, *Vacuum*, Vol. 67, pp. 209-216, ISSN 0042-207X
- Balasundaraprabhu, R; Monakhov, E.; Muthukumarasamy, N.; Nilsen, O & Svensson, B. G. (2009). Effect of heat treatment on ITO film properties and ITO/p-Si interface, *Materials Chemistry and Physics*, Vol. 114, pp. 425- 429, ISSN 0254-0584
- Baojun, Li.; Chua, S. J.; Yakovlev, N.; Lianshan, W.; & Eng-Kee, S. (2003). Properties of Schottky contact of titanium on low doped p-type SiGeC alloy by rapid thermal annealing, *Solid-State Electronics*, Vol. 47, No. 4, pp. 601-605, ISSN 0038-1101
- Benda V.; Gowar J. & Grant D. (1999) *Power Semiconductor Devices: Theory and Applications*, Wiley, ISBN 047197644X, Chichester, England
- Beton, P.H.; Dunn, A.W. & Moriarty P. (1995). Manipulation of C molecules on a Si surface, *Applied Physics Letters*, Vol. 67, pp. 1075 - 1077, ISSN 0003-6951
- Blums J. & Medvid' A. (1995). The Generation of Donor Centres Using Double Frequency of YAG:Nd Laser, *Physics Status Solidi (a)*, Vol. 147, pp. K91-K94, ISSN 1862-6319
- Bruk L.; Fedorov V.; Sherban D.; Simashkevich A.; Usatii I.; Bobeico E. & Morvillo P. (2009). Isotype bifacial silicon solar cells obtained by ITO spray pyrolysis, *Materials Science and Engineering B*, Vol. 159-160, pp. 282-285, ISSN 0921-5107
- Brus L. E. (1984). Electron-electron and electron-hole interactions in small semiconductor crystallites: The size dependence of the lowest excited electronic state, *Journal of Chemical Physics*, Vol. 80, pp. 4403- 4409, ISSN 0021-9606

- Capasso F. (1987). Semiconductors and Semimetals, Chapter 6, Graded-Gap and Superlattice Devices by Bandgap Engineering, Volume 24, 319-395, At&T Bell Laboratories Murray Hill, New Jersey
- Cavallini, A.; Fraboni, B. & Chirco, P. (2000). Electronic properties of traps induced by  $\gamma$ -irradiation in CdTe and CdZnTe detectors, *Nuclear Instruments and Methods in Physics Research Section A: Accelerators, Spectrometers, Detectors and Associated Equipment*, Vol. 448, pp. 558-566, ISSN 0168-9002
- Cavallini, A.; Fraboni, B. & Dusi, W. (2002). Radiation effects on II-VI compound-based detectors, *Nuclear Instruments and Methods in Physics Research Section A: Accelerators, Spectrometers, Detectors and Associated Equipment*, Vol. 476, pp. 770-778, ISSN 0168-9002
- Claeys, C. & Simoen, E. (2007). Germanium-Based Technologies From Materials to Devices, Elsevier, ISBN 978-0-08-044953-1, London
- Crommie, M.F.; Plutz, C. & Eigler, D.M. (1993). Confinement of electrons to quantum corrals on a metal-surface, *Science*, Vol. 262, pp. 218-220, ISSN 0036-8075
- Dumanski L.; Bester M.; Virt I.S. & Kuzma M. (2006). The p-n junction formation in Hg<sub>1-x</sub>Cd<sub>x</sub>Te by laser annealing method, *Applied Surface Science*, Vol. 252, pp. 4481-4485, ISSN 0169-4332
- Evtukh, A.; Medvid, A.; Onufrijevs, P.; Okada, M. & Mimura, H. (2010). Electron field emission from the Si nanostructures formed by laser irradiation, *Journal of Vacuum Science and Technology B: Microelectronics and Nanometer Structures*, Vol. 28., No. 2, pp. C2B11- C2B11, ISSN 1071-1023
- Fougeres, P.; Hage-Ali, M. & Koebel, J.M. (1999). CdTe and Cd<sub>1-x</sub>Zn<sub>x</sub>Te for nuclear detectors: facts and fictions, *Journal of Crystal Growth*, Vol.428, pp. 38-44, ISSN 0022-0248
- Franks, L.A.; Brunett, B.A. & Olsen, R.W. (1999). Radiation damage measurements in room-temperature semiconductor radiation detectors, *Nuclear Instruments and Methods in Physics Research Section A: Accelerators, Spectrometers, Detectors and Associated Equipment*, Vol. 428, pp. 95-105, ISSN 0168-9002
- Fujisawa, I. (1980). Type Conversion of InSb from p to n by Ion bombardment and laser Irradiation. *Japanese Journal of Applied Physics*, Vol. 19, pp. 2137-2140, ISSN 0021-4922
- Gupta R. K.; Yakuphanoglu F.; Ghosh K.& Kahol P. K. (2011). Fabrication and characterization of p-n junctions based on ZnO and CuPc Microelectronic Engineering, *Microelectronic Engineering*, Vol. 88, No. 10, pp. 3067-3069, ISSN 0167-9317
- Junno, T.; Depent, K.; Montelius L. & Samuelson L. (1995). Controlled manipulation of nanoparticles with an atomic-force microscope, *Applied Physics Letters*, Vol. 66., pp. 3627-3629, ISSN 0003-6951
- Kaupuzs J. & Medvid' A. (1994) New Conception in Transistor Technology Using Nonhomogeneous Temperature Field. - Vol. 2335-36, *SPIE Proceedings Microelectronic Manufacturing '94 Conference*, Austin, Texas, USA, October 18-22, pp. 134-145, 1994

- Kiyak S.G. & Savitsky G.V., (1984). Formation of p-n junction on p-type Ge by millisecond laser pulses. *Physics and techniques of semiconductors*, Vol. 18, pp. 1958 – 1964
- Kurbatov, L., Stojanova I., Trohimchuk, P.P. & Trohin, A.S. (1983), Laser annealing of AlInBV compound. *Rep. Acad. Sc. USSR*, Vol. 268, pp. 594- 597, (in Russian);
- Li B.; Chua S.J.; Nikolai Y.; Wang L. & Sia E.K (2003) Properties of Schottky contact of titanium on low doped p-type SiGeC alloy by rapid, *Solid State Electronics*, Vol. 47, pp. 601-605, ISSN 0038-1101
- Lindstrom, G. (2003). Radiation damage in silicon detectors. *Nuclear Instruments and Methods in Physics Research Section A: Accelerators, Spectrometers, Detectors and Associated Equipment*, Vol. 512, pp. 30-43, ISSN 0168-9002
- Ljamichev, I.J.; Litvak, I.I. & N.A. Osvhepkov, Devises on amorphous semiconductors and their application. Moskva, Sov. Radio, 1976.
- Mada, Y. & Ione, N. (1986). p-n junction formation using laser induced donors in silicon, *Applied Physics Letters*, Vol. 48, pp. 1205-1207, ISSN 0003-6951
- Makino T.; Kato H.; Ri S.G.; Yamasaki S. & Okushi H. (2008). Homoepitaxial diamond p-n+ junction with low specific on-resistance and ideal built-in potential *Diamond and Related Materials*, Vol. 17, pp. 782-785, ISSN 0925-9635
- Medvid', A. Fedorenko L. & Frishfelds V. (1998). Electrical properties of donor defects at the surface of InSb after laser irradiation, *Vacuum*, 51, pp. 245 – 249, ISSN 0042-207X
- Medvid', A. & Fedorenko, L. (1999). *Generation of Donor Centers in p-InSb by Laser Radiation*, Materials Science Forum, Vol. 297-298, pp. 311-314, ISSN 0255-5476
- Medvid', A., Litovchenko, V.G., Korbutjak, D., Krilyk, S.G., Fedorenko, L.L. & Hatanaka, Y. (2001). Influence of laser radiation on photoluminescence of CdTe, *Radiation Measurements*, Vol. 33, pp. 725-730, ISSN 1350-4487
- Medvid', A. (2002). Redistribution of the Point Defects in Crystalline Lattice of Semiconductor in Nonhomogeneous Temperature Field, *Defects and Diffusion Forum*, Vol. 210- 212, pp. 89-101, ISSN 1662-9507
- Medvid', A.; Mychko, A.; Fedorenko, L. & Korbutjak, D. (2007). Formation of graded band-gap in CdZnTe by YAG:Nd laser radiation, *Radiation Measurements*, Vol. 42, No. 4-5, pp. 701-703, ISSN 1350-4487
- Medvid', A.; Dmytruk, I.; Onufrijevs, P. & Pundyk, I. (2007). Quantum Confinement Effect in Nanohills Formed on a Surface of Ge by Laser Radiation, *Physica Status Solidi (c)*, Vol. 4, pp. 3066-1069, ISSN 1610-1642
- Medvid', A.; Onufrijevs, P.; Dmytruk, I. & Pundyk, I. (2008). Properties of Nanostructure Formed on SiO<sub>2</sub>/Si Interface by Laser Radiation, *Solid State Phenomena*, Vol. 131-133, pp. 559-562, ISSN 1012-0394
- Medvid', A.; Mychko, A.; Strilchyuk, O.; Litovchenko, N.; Naseka, Yu.; Onufrijev, P. & Pludonis, A. (2008). Exciton quantum confinement effect in nanostructures formed by laser radiation on the the surface of CdZnTe ternary compound, *Physica Status Solidi (c)*, Vol. 6, pp. 209-212, ISSN 1610-1642
- Medvid A.; Onufrijevs P.; Dauksta E.; Barloti J.; Grabovskis D. & Ulyashin A. (2009). Dynamics of Nanostructure Formation using Point Defects on Semiconductors by Laser Radiation, *Physica Status Solidi C*, Vol. 6, pp. 1927-1928, ISSN 1610-1642

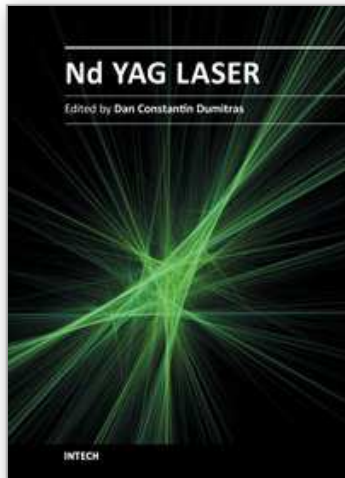
- Medvid', A.; Onufrijevs, P.; Lyutovich, K.; Oehme, M.; Kasper, E.; Dmitruk, N.; Kondratenko, O.; Dmitruk, I. & Pundyk I. (2010). Self-assembly of nanohills in SixGe1-x/Si by laser radiation, *Journal of Nanoscience and Nanotechnology*, Vol. 10, pp. 1094-1098, ISSN 1533-4880
- Medvid', A.; Mychko, A.; Dauksta, E.; Naseka, Y.; Crocco, J. & Dieguez E. Increased Radiation Hardness of CdZnTe by Laser Radiation, *2010 IEEE Nuclear Science Symposium and Medical Imaging Conference*, ISBN 978-1-4244-9106-3, USA, October 2010
- Medvid, A.; Onufrievs, P.; Dauksta, E.; Barloti, J.; Ulyashin, A.; Dmytruk, I. & Pundyk I. (2011). P-n junction formation in ITO/p-Si structure by powerful laser radiation for solar cells applications, *Advanced Materials Research*, Vol. 222, pp. 225-228, ISSN 1022-6680
- Niraula, M.; Mochizuki, D.; Aoki, T.; Hatanaka, Y.; Tomita Y. & Nihashi, T. (1999). Improved spectrometric performance of CdTe radiation detectors in a p-i-n design, *Applied Physics Letters*, Vol.75, pp. 2322-2325, ISSN 0003-6951
- Philipp, H.P. & Taft, E.A. (1959). Optical constants of germanium in the region 1 to10 eV, *Physical Review*, Vol. 113, No. 4, pp. 1002-1005
- Pozela J. (1980) *Semiconductor Transducers*, Mokslas, Vilnius
- Romanov, V. & Serdega, B. (1975). Bipolar electric conductivity of germanium in a high-frequency electric field, *Physics and technics of semiconductors*, Vol. 9, No.4, pp. 665 - 668.
- Shapiro, J. (2002). *Radiation protection: a guide for scientists, regulators, and physicians*, 4th ed., Harvard college
- Shaw, D. (1973). *Atomic Diffusion in Semiconductors*, Plenum Press, London and New York
- Suzuki, K.; Seto, S.; Savada, T.; Imai, K.; Adachi, M. & Inabe, K. (2001). Photoluminescence measurements on undoped CdZnTe grown by the high-pressure Bridgman method, *Journal of Electronic Materials*, Vol.30 pp. 603-607, ISSN 0361-5235
- Taguchi, T.; Shirafuji, J. & Inuishi, Y. (1978). Gamma and electron radiation effects in CdTe, *Nuclear Instruments and Methods in Physics Research Section A: Accelerators, Spectrometers, Detectors and Associated Equipment*, Vol.150, pp.43-48, ISSN 0168-9002
- Tomas A.P.; Jennings M.R.; Davis M.; Shah V.; Grasby T. & Covington J.A. (2007). High doped MBE Si p-n and n-n heterojunction diodes on 4H-SiC, *Microelectronics Journal*, Vol. 38, No. 12, pp. 1233-1237, ISSN 0026-2692
- Toshiharu M.; Hiromitsu K.; Sung-Gi Ria, Satoshi Y. & Hideyo, O. (2008). Homoepitaxial diamond p-n+ junction with low specific on-resistance and ideal built-in potential, *Diamond & Related materials*, Vol. 17, pp. 782 - 785, ISSN 09259635
- Tovstyuk, K.D.; Placko, G.V.; Orletskiy, V.D.; Kiyak, S.G. & Babytskiy, J. V. (1976). The formation of p-n and n-p-junction in semiconductor by laser radiation, *Ukrainian Journal of Physics*, Vol. 21, 1918 - 1920.
- Vu, V. T.; Nguyen, D. C.; Pham, H. D.; Chu, A. T. & Pham, T. H. (2010). Fabrication of a silicon nanostructure-based light emitting device, *Advances in natural sciences: nanoscience and nanotechnology*, Vol. 1, pp. 025006-025010, ISSN 2043-6254



Yang, G.; Jie, W. & Zhang, Q. (2006). Photoluminescence investigation of CdZnTe:In single crystals annealed in CdZn vapors *Japanese Journal of Applied Physics*, Vol.21 pp.1807-1809, ISSN 0021-4922

IntechOpen

IntechOpen



## **Nd YAG Laser**

Edited by Dr. Dan C. Dumitras

ISBN 978-953-51-0105-5

Hard cover, 318 pages

**Publisher** InTech

**Published online** 09, March, 2012

**Published in print edition** March, 2012

Discovered almost fifty years ago at Bell Labs (1964), the Nd:YAG laser has undergone an enormous evolution in the years, being now widely used in both basic research and technological applications. Nd:YAG Laser covers a wide range of topics, from new systems (diode pumping, short pulse generation) and components (a new semiorganic nonlinear crystal) to applications in material processing (coating, welding, polishing, drilling, processing of metallic thin films), medicine (treatment, drug administration) and other various fields (semiconductor nanotechnology, plasma spectroscopy, laser induced breakdown spectroscopy).

### **How to reference**

In order to correctly reference this scholarly work, feel free to copy and paste the following:

Artur Medvid', Aleksandr Mycko, Pavels Onufrijevs and Edvins Dauksta (2012). Application of Nd:YAG Laser in Semiconductors' Nanotechnology, Nd YAG Laser, Dr. Dan C. Dumitras (Ed.), ISBN: 978-953-51-0105-5, InTech, Available from: <http://www.intechopen.com/books/nd-yag-laser/application-of-nd-yag-laser-in-semiconductors-nanotechnology>

**INTECH**  
open science | open minds

### **InTech Europe**

University Campus STeP Ri  
Slavka Krautzeka 83/A  
51000 Rijeka, Croatia  
Phone: +385 (51) 770 447  
Fax: +385 (51) 686 166  
[www.intechopen.com](http://www.intechopen.com)

### **InTech China**

Unit 405, Office Block, Hotel Equatorial Shanghai  
No.65, Yan An Road (West), Shanghai, 200040, China  
中国上海市延安西路65号上海国际贵都大饭店办公楼405单元  
Phone: +86-21-62489820  
Fax: +86-21-62489821

© 2012 The Author(s). Licensee IntechOpen. This is an open access article distributed under the terms of the [Creative Commons Attribution 3.0 License](#), which permits unrestricted use, distribution, and reproduction in any medium, provided the original work is properly cited.

IntechOpen

IntechOpen